

Approved for public release: distribution unlimited.

Wave Energy Resource Characterization for San Nicholas Island

by Noah Johnson and Jim Thomson

Technical Memorandum

APL-UW TM 3-18

June 2018



Applied Physics Laboratory University of Washington
1013 NE 40th Street Seattle, Washington 98105-6698

Award: N00024-10-D-63

AUTHORSHIP NOTE

This report was written during spring quarter 2018 by Noah Johnson, a senior in undergraduate study at the University of Washington, in fulfillment of 4 credits of independent study for Mechanical Engineer 499. Jim Thomson collected the original data and was the advisor for the independent study.

ABSTRACT

To characterize the wave energy resource for San Nicolas Island, off the coast of Southern California, wave data collected on three buoys located near the island were assembled from the Coastal Data Information Program (CDIP). These data were used to create joint probability density function plots and monthly-averaged plots of bulk parameters and energy spectra. Observed monthly-averaged bulk parameters and calculated power densities were compared to a wave energy atlas created by the National Renewable Energy Laboratory (NREL). Wave climatology products available from the Global Spectral Wave Climate (GLOSWAC) program were also compared with the climatology derived from the buoy data. Finally, regional spatial gradients in wave height and energy period were quantified using the difference between drifting Surface Wave Instrument Float with Tracking (SWIFT) measurements and the moored buoys, including a comparison of atlas values for these spatial gradients. In general, the atlas values agree well with the CDIP buoy data for significant wave height, but overestimate energy period and fail to capture wave direction trends. The atlas values overestimate observed power densities within a standard deviation of the observed values and capture observed variation in power density between different CDIP buoy locations. The atlas values underestimate observed spatial gradients for significant wave height and fail to capture observed spatial gradients for energy period.

TABLE OF CONTENTS

1.	Introduction	1
2.	Buoy Data	2
2.1	Data Assembly and Overview	3
2.2	Bulk Parameters	5
2.3	Energy Spectra	8
2.4	Joint Probability Density Functions	9
3.	NREL Wave Energy Atlas Comparison	10
3.1	Atlas Background.....	10
3.2	Bulk Parameters	11
3.3	Power Density	12
4.	Wave Climatology Using GLOSWAC	14
4.1	Background	15
4.2	Discussion	15
5.	Spatial Gradients Case Study	18
5.1	Gradient Comparison Methodology	18
5.2	Sea State During SWIFT Deployment.....	19
5.3	Spatial Gradient Comparison: Significant Wave Height	20
5.4	Spatial Gradient Comparison: Energy Period.....	22
6.	References	23
7.	Appendix: Accessing Data from THREDDS Server and CDIP Website	24

1. INTRODUCTION

Wave energy resource characterizations offer quantitative and qualitative descriptions of a wave energy resource, often for a specific location. Ideally, characterization uses in situ data such as buoys that record raw wave motions, and data sets are several years in duration. The raw buoy motions are processed in 30-min or less windows so that the underlying sea state has statistical stationarity (i.e., conditions do not change within those 30 min). The processing reduces the raw data to spectral energy densities and directional moments as a function of wave frequency. Statistical or “bulk” parameters usually calculated from the spectra include significant wave height (H_s), peak period (T_p), energy period (T_e), peak direction (D_p), and power density (P).

Significant wave height represents the average height of the largest third of waves. Peak period is the period corresponding to the maximum level in an energy spectrum. Peak direction is the direction corresponding to the peak in an energy spectrum. The energy period T_e is a weighted calculation of period from an energy spectrum:

$$T_e = \frac{\int E(f)df}{\int fE(f)df} = \frac{\sum E_i}{\sum f_i E_i} \quad (1)$$

where E is the wave energy density (m^2/Hz) and f is frequency (Hz) [1]. Wave power density, a principal quantitative measurement of interest, is calculated by multiplying a sea state’s energy by its group velocity. The equation for wave power density is:

$$\bar{P} = \bar{E}c_g = \frac{1}{16}\rho g H_s^2 \left(\frac{L}{2T_e} + \frac{2\pi d}{T_e \sinh(4\pi d/L)} \right) \quad (2)$$

where E is the energy density, c_g the group velocity at the energy period, ρ the density of water, g the gravitational acceleration, H_s the significant wave height, L the wavelength, T_e the energy period, and d the water depth [2]. Wavelength L was determined by iterative process solving the wave dispersion relation for intermediate water depth. In this report, wavelength was calculated using an iterative MATLAB function with inputs of energy period and depth.

The U.S. Department of Energy (DOE) commissioned an assessment of the nation’s wave energy resources. The Virginia Tech Advanced Research Institute (VT-ARI) partnered with the Electric Power Research Institute (EPRI) and the National Renewable Energy Lab (NREL) to produce a report detailing the wave energy assessment and methodology. The wave energy assessment was combined with several other marine energy products to create the Marine and Hydrokinetic Atlas hosted online by NREL.

The basis of the model is a 51-month data set of hindcast results produced by the National Oceanic and Atmospheric Administration National Center for Environmental Prediction (NOAA NCEP) that contains over 42,000 output grid points from the WAVEWATCH III model [3]. To create the atlas, spectra were reconstructed with modified gamma spectra having two spectral shape coefficients, where the coefficients were selected to best fit full hindcast spectra from deep water calibration stations for each of the 51 months that informed the model. The calibration stations include 15 stations selected from 257 WAVEWATCH III sites with archived directional spectra. VT-ARI researchers cite differences between the model and buoy data that likely result from missing buoy data or regional bias, because buoys are more often damaged and offline in winter. This results in underreporting if the average is taken of remaining samples. The wave power densities in the atlas include average annual and 12 monthly scalar wave power densities (kW/m of wave crest width across a unit diameter circle) [3]. The spectral shape coefficients are not available.

The National Research Council (NRC) reviewed the wave energy assessment methodology and concludes that the model performs poorly in shallow water and relies on a limited data set. The NRC also suggests that assessors distinguish between scalar (unit-circle) and directional approaches to estimate wave power density. Particularly, the NRC report notes that summation of scalar power densities along a coastline is not a valid method for determining the total available power; rather, the component of wave power normal to the coast must be used [4].

A wave energy assessment for the United Kingdom was produced by the Crown Estate with contributions by Black and Veatch Ltd. This UK assessment focused on the offshore rather than the nearshore resource because the offshore is easier to model and more likely to be harvested due to economic, social, and political factors. The assessment established “Key Resource Areas” where power density was greater than 20 kW/m and concludes that regeneration nearshore after offshore harvesting was not feasible due to the large regeneration scales (i.e., fetch) that would be required. The report also discusses farm scale and shadow effects that can alter the recoverable resource [5].

Here, we focus exclusively on characterization of the wave energy resource at a specific location and do not offer advice on implementation. This report uses the NREL Wave Energy Atlas and evaluates its usefulness as a tool for wave resource assessments at regional scales.

2. BUOY DATA

Wave data from three buoys near San Nicolas Island were assembled and analyzed to produce a sea state climatology for the region. The buoy data were used to create monthly-averaged plots of bulk parameters and energy spectra. Plots of joint probability density functions for bulk parameters were also created. The buoy data were available from the Coastal Data Information Program (CDIP), which maintains two of the three buoys used in this analysis. The third buoy was deployed by the Applied Physics Laboratory of the University of Washington (APL-UW) for two years, as part of a project

funded by the Naval Facilities and Engineering Command (NAVFAC). These data are also available in the CDIP archive, as part of a long-standing partnership between APL-UW and CDIP.

2.1 Data Assembly and Overview

San Nicolas Island is one of the Channel Islands off the Southern California coast and is controlled by the United States Navy. All available historical sea state data from three buoys near San Nicolas Island (Table 1; Figure 1) were retrieved from the CDIP website.



Figure 1. Area of interest (left) and position of relevant buoys (right)

Table 1. Buoy Information Summary

Name	Station	Operator	Status
San Nicolas Island, CA	067	Navy	Active
Begg Rock, CA	138	APL-UW	Decommissioned
San Nicolas Island Barge Landing, CA	140	Navy	Decommissioned

The CDIP data records for the three buoys of interest from 1982 to the present only overlap occasionally (Figure 2). Wave height, period, and direction for the three buoys were plotted as a function of time (Figures 3–5).

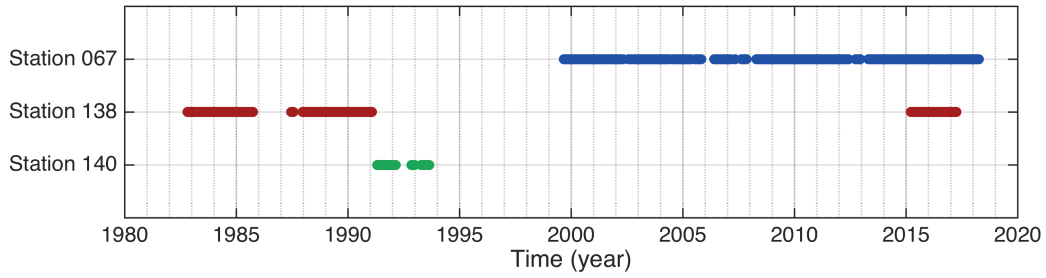


Figure 2. Time-availability of sea state data from selected buoys

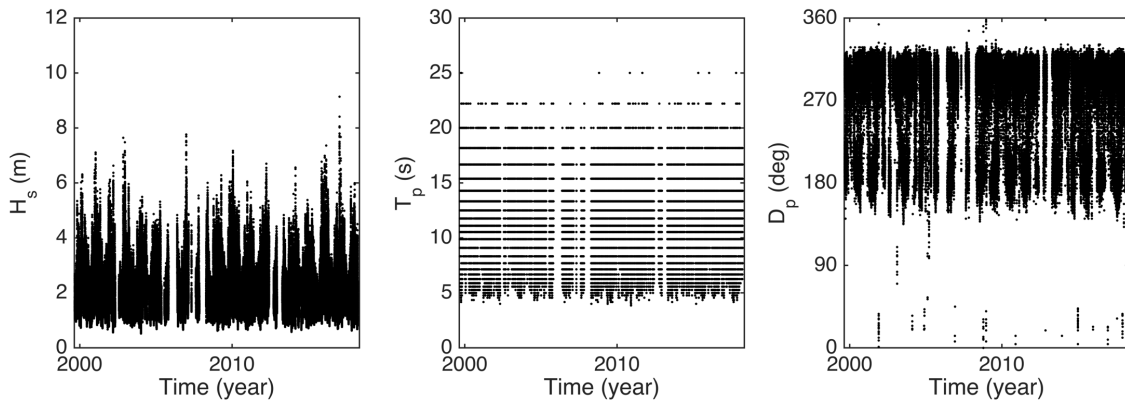


Figure 3. Time series sea state data for buoy CDIP Station 067, San Nicolas Island

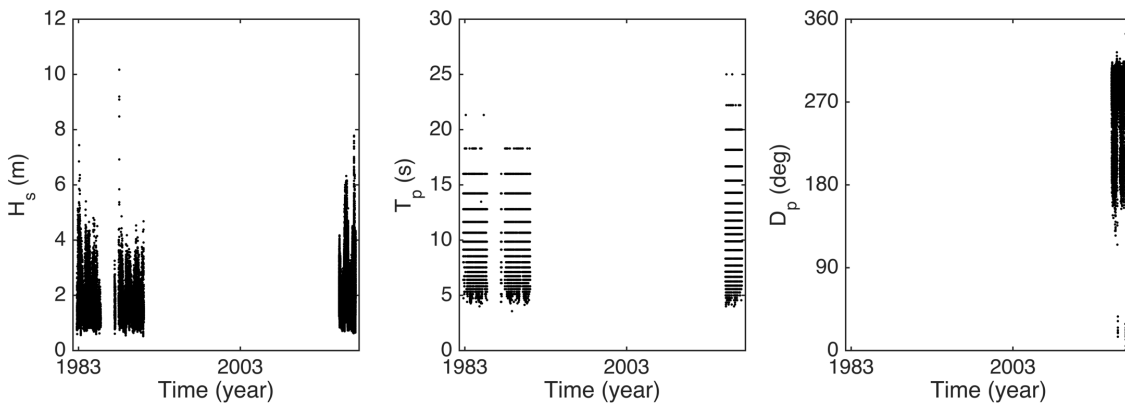


Figure 4. Time series sea state data for buoy CDIP Station 138, Begg Rock

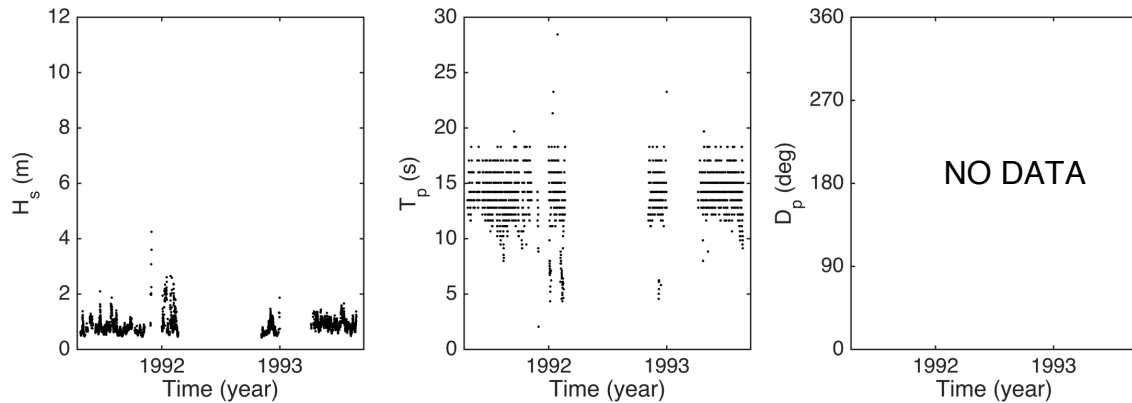


Figure 5. Time series sea state data for buoy CDIP Station 140, Barge Landing

Station 067 generally has waves with significant heights of 0.5–8 m, periods of 5–25 s, and directions of 160–330° with greater concentration in the range 270–330°. Data available from this buoy span 1999–2018 with few gaps.

Station 138 generally has waves with significant heights of 0.5–6 m, periods of 5–20 s, and directions of 160–330°. Data available from this buoy include the 1980s and 2010s. Direction data are limited to the 2010s deployment.

Station 140 generally has waves with significant heights of 0–2 m and periods of 10–20 s. No directional data are available for this buoy. Data available from this buoy span 1991–1993, with several gaps.

Wave heights are slightly greater for Station 067 than for Station 138, likely due to the generally greater exposure of Station 067 and because the buoy is at the transition between deep and shallow water (Figure 1). Wave heights are less for Station 140 compared to Stations 067 and 138, likely due to its position on the leeward side of San Nicolas Island.

Wave periods for Station 140 may be lacking below 10 s compared to Stations 067 and 138, again due to its leeward position that may prevent shorter-period local wind-driven waves from reaching the buoy.

For all buoys, the striped nature of the peak period T_p is the result of discrete frequency bands in the calculated energy spectra. The frequency bands are linear, and thus the periods (equal to the inverse of frequencies) are spaced logarithmically. This discretization effect can be mitigated in the calculation of energy period T_e .

2.2 Bulk Parameters

Bulk parameters were separated into one-month bins and averaged for each month, resulting in plots of significant wave height, peak period, and direction as functions of month for each of the three stations (Figure 6).

The monthly-averaged wave parameters have similar ranges in wave height for Stations 067 and 138, although the decrease in wave height during summer for Station 138 is more prolonged and slightly greater. Stations 067 and 138 have maximum monthly-averaged wave heights from November to April and minimums in August. Station 140 has a less recognizable pattern in monthly-averaged wave heights, decreasing slightly during October, though the variation in significant wave height is small when compared to the other stations. The absolute maximum significant wave height for Stations 067 and 138 is approximately 10 m, while the absolute maximum wave height at Station 140 is approximately 4 m. The occurrence of these maximum events in winter is expected. Variance in wave height for Stations 067 and 138 is generally less than ± 1 m, and decreases during summer. Wave height variance for Station 140 is generally less than ± 0.5 m.

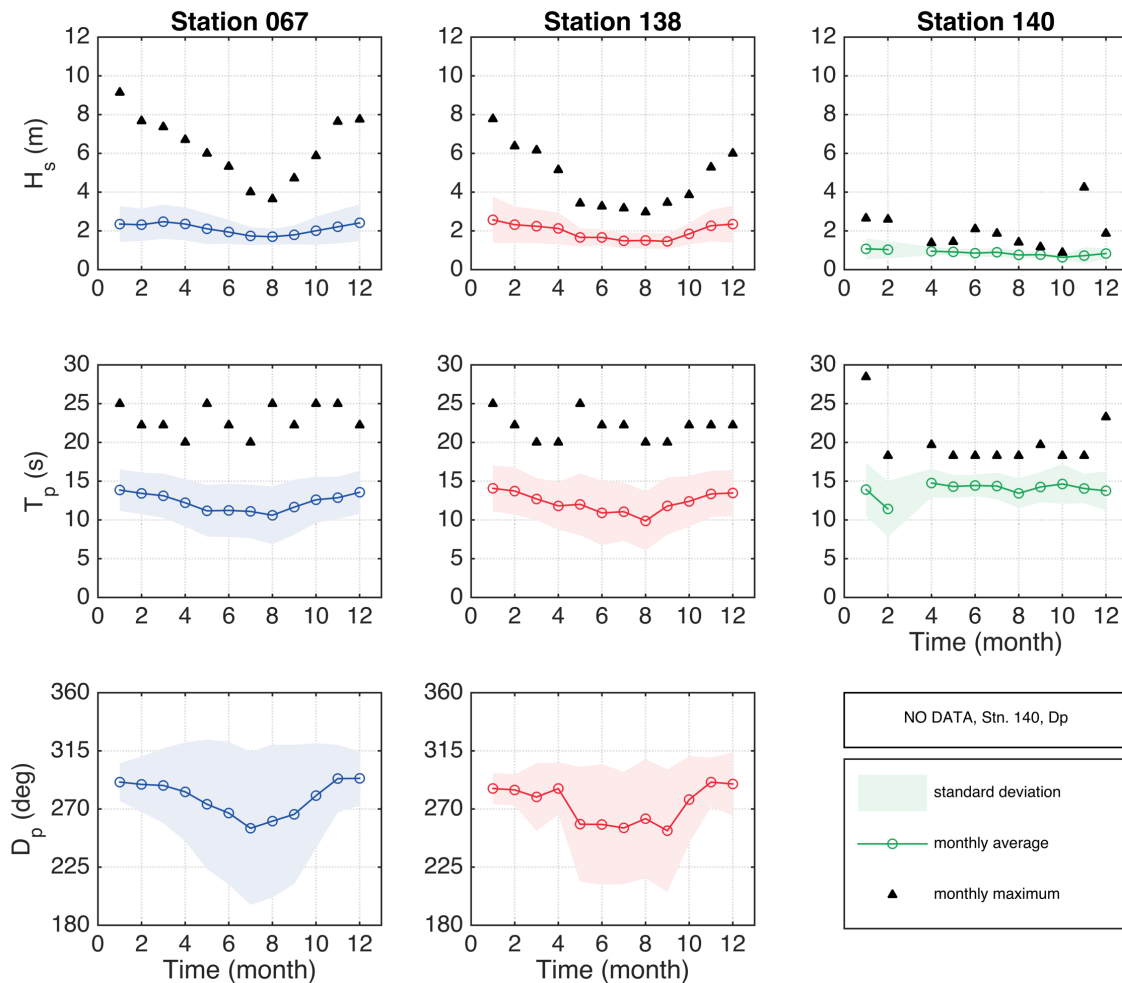


Figure 6. Monthly-averaged bulk parameters with standard deviations and maximums

Monthly-averaged peak period has similar trends to those for wave height. Stations 067 and 138 are similar, while Station 140 has only small variations in peak period throughout the year. Station 140 generally retains longer-period waves (15 s), likely because longer-period waves refract around the island to the more sheltered location of Station 140. Variance in peak period for Stations 067 and 138 is less than ± 5 s for all months and increases slightly during summer. The variance in peak period for Station 140 is generally less than at the other stations, but caution should be taken in interpreting this result because the data set for Station 140 is smaller than the other stations.

Monthly-averaged direction remains around 270° throughout the year for Stations 067 and 138, with small decreases in angle from approximately April to October. Variance in wave direction increases in summer to approximately $\pm 60^\circ$ for Station 067 and approximately $\pm 45^\circ$ for Station 138. No wave direction data are available for Station 140. Note that wave direction data are available only during the 2015–2017 deployments for Station 138.

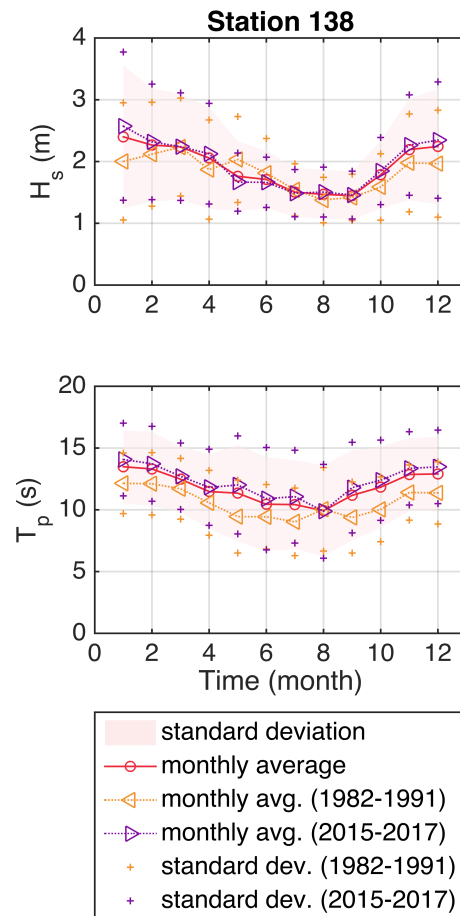


Figure 7. Comparison of historical data for Station 138

Considering monthly-averaged values for significant wave height and peak period at Station 138 over two data periods, 1982–1991 and 2015–2017, shows that they are in good agreement (Figures 6 and 7). In general, the monthly-averaged significant wave height over 2015–2017 is greater during winter than that for the period 1982–1991. This may be due to a strong El Niño event during 2015 that would increase wave heights off the Southern California coast; however, El Niño events also occurred in 1982, 1987, and 1991 [6]. The same pattern is apparent for peak wave period, but to a greater degree; monthly-averaged peak period over 2015–2017 is consistently greater than the average values for the period 1982–1991. These differences are likely attributed to the higher-fidelity measurements of the more recent deployment, although other, more complex causes are also likely.

2.3 Energy Spectra

Average energy spectra for each month of the year for all data sets from the three San Nicolas Island buoys (CDIP 067, 138, 140) were calculated from the wave energy spectra, which were accessed on the CDIP website. For Stations 067 and 138, spectra were retrieved directly through MATLAB using the THREDDs server. Spectra for Station 140 were unavailable on the server; download required a visit the CDIP website. (Download procedures are given in the Appendix.) Spectra were organized and the mean energy density was calculated for each frequency bin for every month (Figure 8).

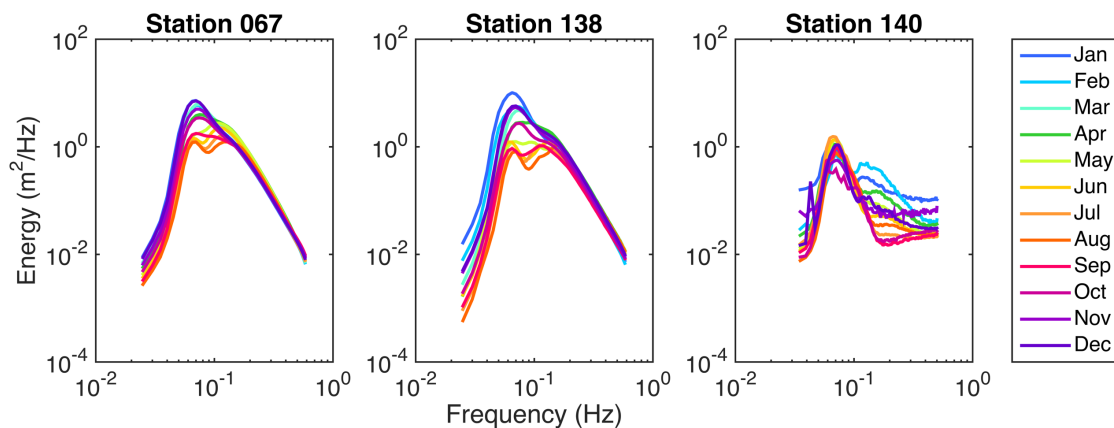


Figure 8. Monthly-averaged energy spectra for the three wave buoys

Stations 067 and 138 have more pronounced spectral peaks during winter, as expected. Station 138 has a greater annual energy density variance in lower frequencies than Station 067. Station 138 appears to have a greater winter peak energy density variance than Station 067. Stations 067 and 138 have a clear equilibrium range with dependence of frequency to the power -4 at high frequencies [7]. Station 140 lacks this

equilibrium range, probably because of insufficient frequency response in the older buoys at this site.

2.4 Joint Probability Density Functions

Joint probability density function (PDF) plots of wave height as a function of three different wave periods: energy period, average period, and peak period, were calculated from bulk parameter data (Figure 9). During the spectral data organization, the energy period for every spectrum was also calculated. The energy period was used to create joint PDFs for significant wave height (H_s) and energy period (T_e). These plots are supplemented with plots developed for wave height with respect to average period (T_a) and peak period (T_p).

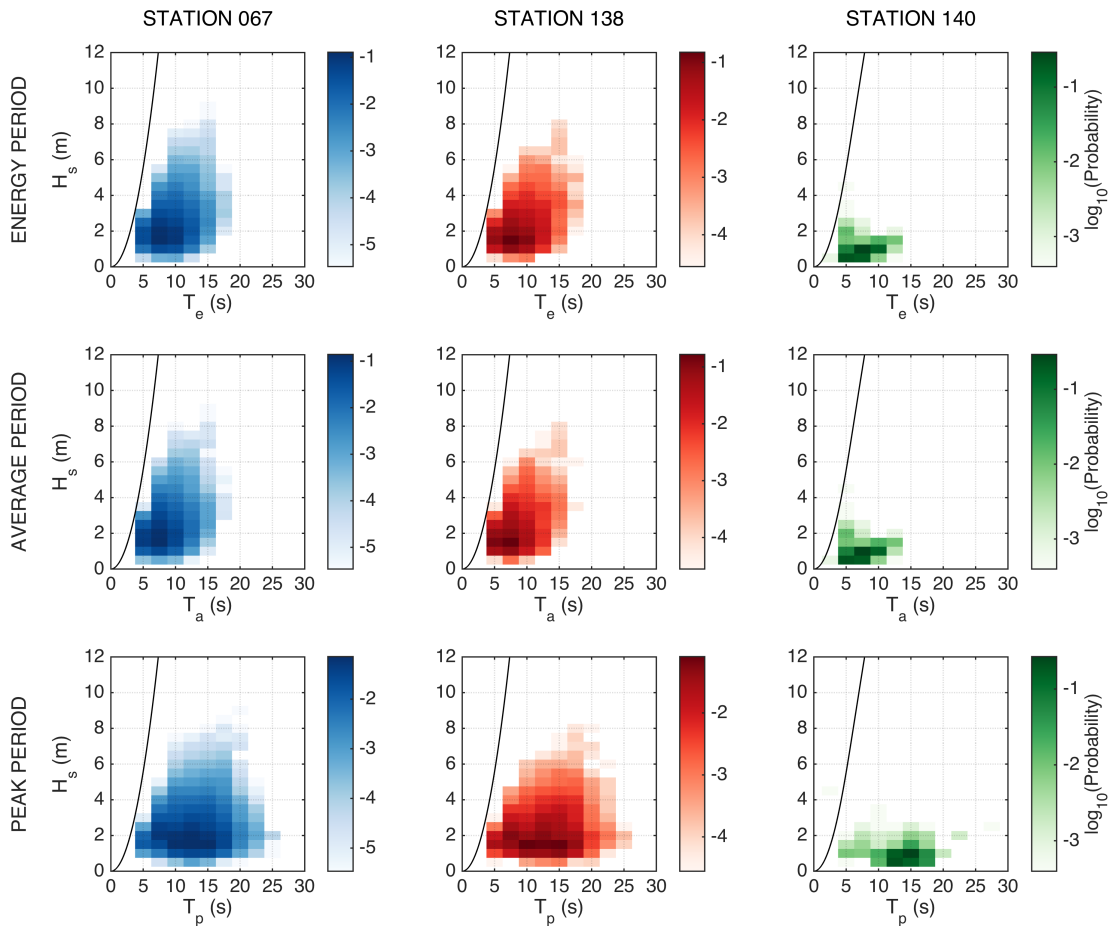


Figure 9. Joint probability density functions, period comparison, where increasing color intensity represents increasing of the base-10 logarithm of the normalized probability. A steepness limit curve is also shown on all plots using a wave steepness limit of $H/L = 1/7$.

PDF plots for Station 067 show that the average period and energy period plots have a narrower data spread and are concentrated at smaller periods. This observation is expected; peak period is generally at longer periods because it disregards the wind-sea distribution located at shorter wavelengths (higher frequencies). The energy period concentration is located at a marginally longer period than the average period plot, though the differences are small. Observations for all three stations agree well.

Stations 067 and 138 have a greatest probability of waves with an average period of approximately 5 s and significant wave height of 1.5–2 m; Station 140 has a high probability of waves with an average period of 5–10 s and significant wave height of 0.5–1 m. The value for the average period cluster is generally smaller than the value for the peak period cluster due to the uneven distribution of wave periods about the peak period caused by local wind-driven sea states, which shifts the average period to smaller values.

Stations 067 and 138 have a high probability of waves with peak period of 15 s and significant wave height of 1.5–2 m. Station 140 has a high probability for waves with peak period of 15 s and a significant wave height of approximately 1 m.

3. NREL WAVE ENERGY ATLAS COMPARISON

Wave climatology retrieved from the NREL wave energy atlas was compared to wave climatology calculated from the buoy measurements, primarily using monthly-averaged significant wave height, energy period, and direction for the three stations (067, 138, 140). A comparison was also made between power density values calculated from observed data and values retrieved from the atlas. In general, the atlas compares well with the CDIP buoy data for significant wave height, but it overestimates energy period and fails to capture wave direction trends. The atlas tends to overestimate observed power densities, but the estimates are within one standard deviation of the observed values and capture observed variation in power density between different CDIP buoy locations.

3.1 Atlas Background

The NREL hosts the Marine and Hydrokinetic (MHK) Atlas (<https://maps.nrel.gov/mhk-atlas>), which offers resource estimates for multiple MHK technologies including wave energy. The wave energy atlas was produced jointly by EPRI and Virginia Tech for the DOE. The assessment group used a wave hindcast produced by the NOAA NCEP using WAVEWATCH III. The version of WAVEWATCH III used to produce the wave energy atlas was limited to deep water because it does not perform well in shallow water (< 50 m).

Wave climatology available through the wave energy atlas includes monthly-averaged and annually-averaged values for significant wave height, energy period, direction, and power density. Monthly-averaged values were recorded manually from the online map interface by selecting points as close as possible to the buoy coordinates and transcribing the parameter magnitudes.

3.2 Bulk Parameters

The monthly-averaged values from the atlas were plotted with the monthly-averaged values retrieved from historical CDIP buoy data (Figure 10). Shaded error bars are included for the CDIP buoy data. No statistical range is provided from the atlas.

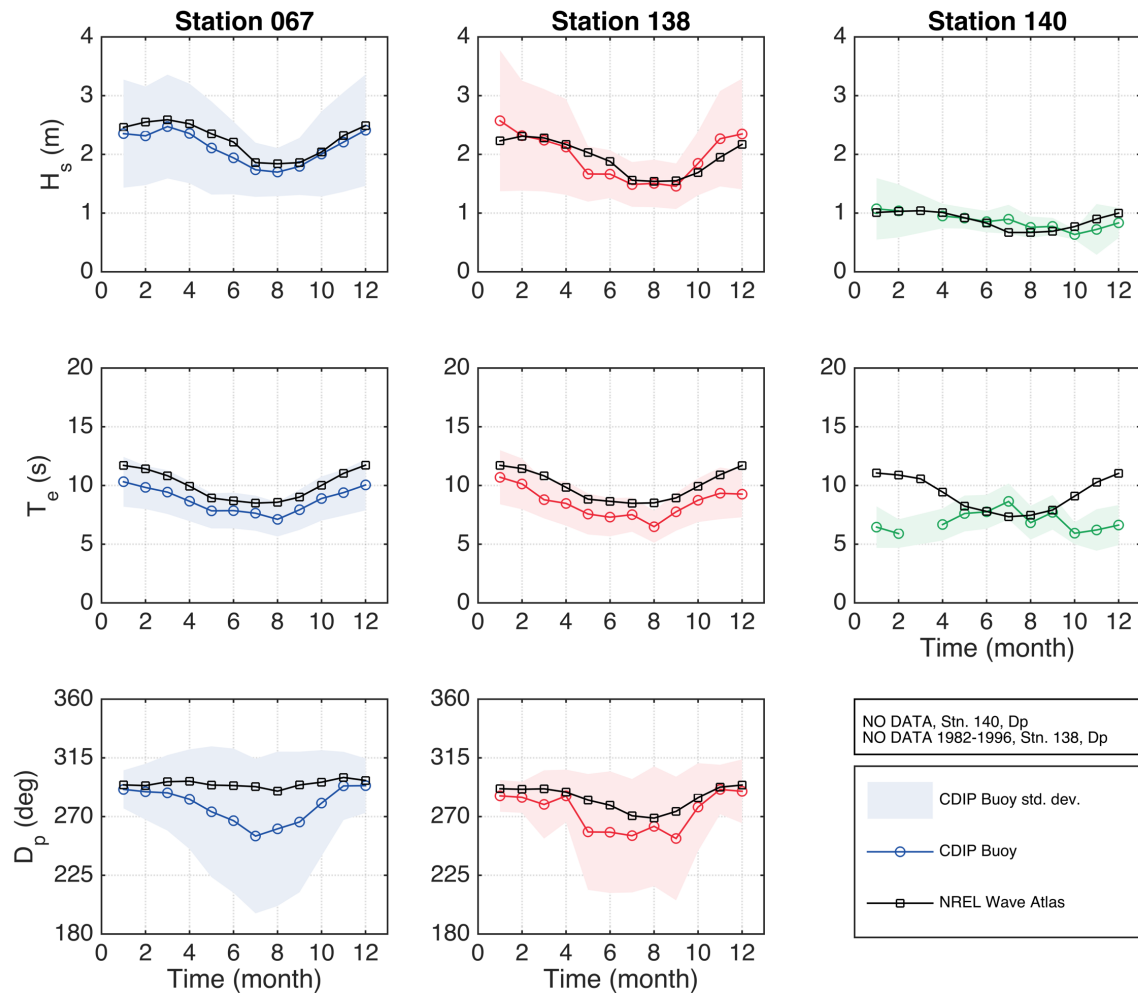


Figure 10. Monthly-averaged parameter comparison

The atlas and CDIP buoy data are in good agreement for significant wave height, but the atlas overestimates energy period and fails to capture wave direction trends. The atlas and CDIP buoy data for significant wave heights are within one standard deviation for all stations. The National Research Council evaluation report on the wave energy resource assessment used in the atlas recognizes that the WAVEWATCH III models

wave height well, because wave height has been the primary metric used for model tuning [4].

The energy periods produced by the atlas consistently overestimate the buoy data from Stations 067 and 138 by approximately 1–2 s. Generally, for Stations 067 and 138, the atlas values for energy period are approximately one standard deviation above the CDIP buoy data. The energy period curves produced by the atlas for the three stations are similar, suggesting that the model might not be well resolved with respect to energy period or that the spectral fitting method has a systematic bias. Some of the significant variation in the energy period comparison for Station 140 may be attributed to the limited data available from the CDIP buoy, and perhaps more significantly, the shallow depth (18.3 m) at the buoy location. The shallow water at Station 140 places the buoy within the questionable WAVEWATCH III output range.

The atlas direction data differ from the buoy measurements and fail to account for significant declinations in wave direction during summer, as observed especially for Station 067. Direction values were not always available from the atlas at the exact matching point. Direction values were taken from the nearest point for which direction data exist, and this may introduce errors where there are significant depth gradients. The lack of resolved direction data may also contribute to the differences in direction between the atlas and the buoy measurements. For Stations 067 and 138, the atlas direction data are within one standard deviation of the buoy data. No direction data exist from the CDIP buoy for Station 140 and thus the atlas results for this station were omitted.

Overall, the NREL wave energy atlas agrees well with the buoy data for monthly-averaged significant wave height, but overestimates the energy period and agrees poorly with the buoy direction data. Furthermore, the atlas appears to perform poorly in shallow water (see Station 140) as expected due to the WAVEWATCH III constraints to deep water. The National Research Council report on the methods used to create the wave atlas suggest that errors in the atlas may stem from “... (1) inaccuracies in the WAVEWATCH III simulations and (2) differences between the full and reconstructed wave spectra.” [4] These errors may further contribute to the dissimilarities between the atlas and the historical CDIP buoy data.

3.3 Power Density

Average power densities were calculated by month for each of the three CDIP buoy sites surrounding San Nicolas Island. First, the power density was calculated for all data points using Eq. (2), then averaged in their respective monthly bins.

Power density is maximum in winter and is minimum in August for all three stations, confirming the seasonal variability of the site (Figure 11). The standard deviation for power density is greatest in winter, as expected, because power density scales with the square of significant wave height, which also has a greater range in winter. Power density magnitudes are slightly greater at Station 067, where increased wave exposure results in greater significant wave heights than at Station 138. Station 140

has very low power density magnitudes due to the small significant wave height observed at this station.

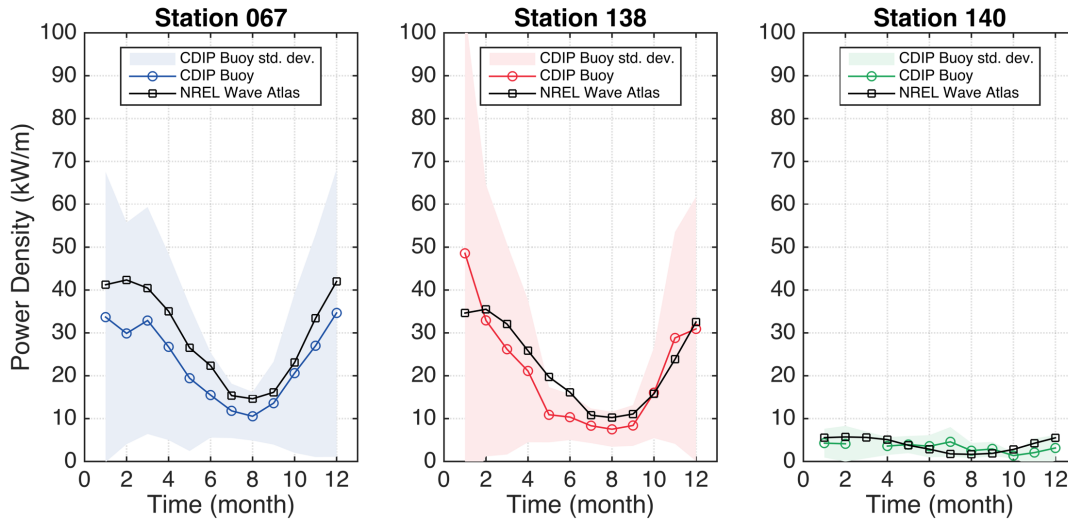


Figure 11. Comparison of observed and atlas power densities

The atlas results (Figure 11, black curves) tend to overestimate the observed monthly-averaged power densities. However, the atlas performs relatively well and is within one standard deviation of the observed values. The atlas data capture well the local variation between Stations 138 and 140, where power densities differ greatly.

Note that if monthly-averaged power densities were calculated using the monthly-averaged significant wave height and monthly-averaged energy period (incorrect) the results would differ from the approach taken in this report, which is to calculate *all* power densities *then* average by month.

Comparing the two power density calculation methods shows that the incorrect method (Figure 12, solid markers) always underestimates the correct power densities (transparent markers). This difference can be understood by knowing that Eq. (2) includes and is driven by the term H_s^2 and that the incorrect method squares the monthly-averaged significant wave height, whereas the correct method squares all significant wave heights and then averages the result. The average of the squares of a set of non-uniform values will always be greater than the square of the average of the same values, leading to a gap in the results between the two methods (Figure 12). The difference is greater in winter because the significant wave heights are greater in winter, increasing the impact of squaring first before averaging.

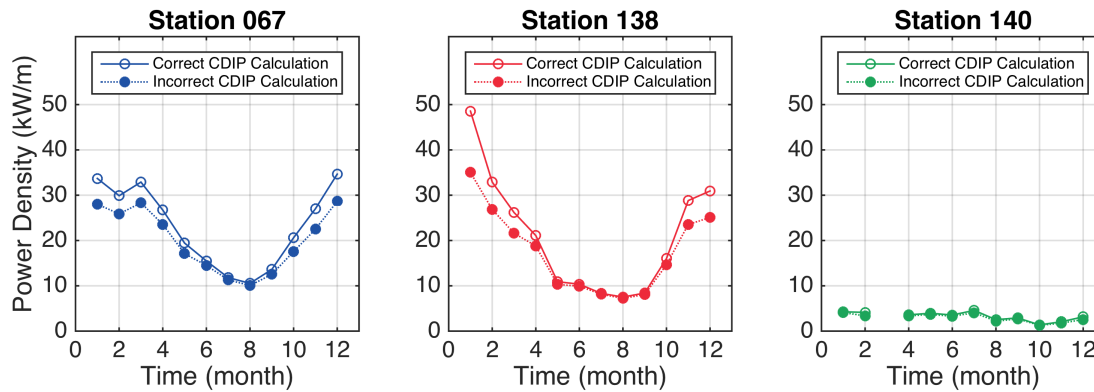


Figure 12. Comparison of power density calculation methods

The atlas also reports an annual average power density that can be compared to the average annual power density calculated as the average of the observed monthly averages (Figure 11).

The comparison of the atlas and observed average annual power densities (Table 2) shows that the NREL atlas overestimates the average annual wave power density for the three locations around San Nicolas Island. This is consistent with the overestimation of monthly-average wave power density (Figure 11). The error between the atlas and observed values, taking the observed value as the “true value,” results in percent errors of 28, 7, and 18 percent for stations 067, 138, and 140, respectively.

Table 2. Comparison of Atlas and Observed Annual Average Power Density

Location	Average Annual Wave Power Density		
	Atlas (kW/m)	Observed (kW/m)	Error (%)
Station 067	29.38	23.03	28
Station 138	22.35	20.84	7
Station 140	3.88	3.28	18

4. WAVE CLIMATOLOGY USING GLOSWAC

Products available from an online wave climatology resource were analyzed in the context of the sea states for the three stations near San Nicholas Island. The Global Spectral Wave Climate (GLOSWAC) system uses a spectral partitioning method to quantify common wave systems at a location, thereby providing a more physical climatology than simply averaging all observations (i.e., all wave systems) [8].

4.1 Background

The GLOSWAC website (<http://improlife.xyz/>) offers parameterized wave data in multiple graphical representations based on model wave spectra from the ERA-Interim reanalysis project. The grid resolution is approximately 100 km and a search for a latitude and longitude within the map will redirect to the nearest grid point. Station 067 corresponds to a unique grid point. Stations 138 and 140 share a grid point due to their proximity.

The plots sourced from GLOSWAC include “Spectral Statistics and Wave Systems” (Figure 13a and d), “Significant Wave Height Distribution Per Wave System” (Figure 13b and e), and “Monthly Mean Significant Wave Height” (Figure 13c and f).

4.2 Discussion

GLOSWAC data points do not match geographically with the buoy coordinates (Figure 14). The GLOSWAC data point used for Station 067 is nearly 55 km to the west of the buoy, while the GLOSWAC data point used for Stations 138 and 140 is nearly 60 km to the southeast of Station 138 and nearly 40 km to the southeast of Station 140. For reference, all buoys are less than 40 km from San Nicolas Island. Thus, comparisons between GLOSWAC results and observed data are made with caution.

GLOSWAC “Spectral Statistics and Wave Systems” plots identify different wave systems using the “mountaineer scheme” where local peaks are identified with gradients (Figure 13a and d). The different wave systems generally refer to distinct types of meteorological events that can be partitioned for a specific location. For Station 067 there are four distinct wave systems: two originating predominately from the south and two originating predominately from the northwest. The plot produced for the data point nearest Stations 138 and 140 has six distinct wave system partitions, with slightly more western origins. Only one wave system is identified originating from the south, while there are four partitions for wave systems originating from the northwest. An additional, smaller wave system appears to originate from the east (labeled as system 6 in Figure 13d). Note that small changes in the spectrum can create significant variation in how many unique events are classified, which may alter interpretation.

Wave system 1 is highly concentrated and originates in the Southern Ocean (Figure 13a and d). This is supported by the plots (Figure 13c and f) where wave system 1 shows waves with greatest monthly average significant wave height from May through September, corresponding to winter in the Southern Hemisphere and thus larger swells arriving from the south. Systems 2 and 3 in Figure 13a and systems 2–5 in Figure 13d show swell from the North Pacific that is less concentrated than swell from the Southern Ocean. This is supported by the monthly average wave heights (Figure 13c and f) that show a pattern of wave heights corresponding to winter in the Northern Hemisphere.

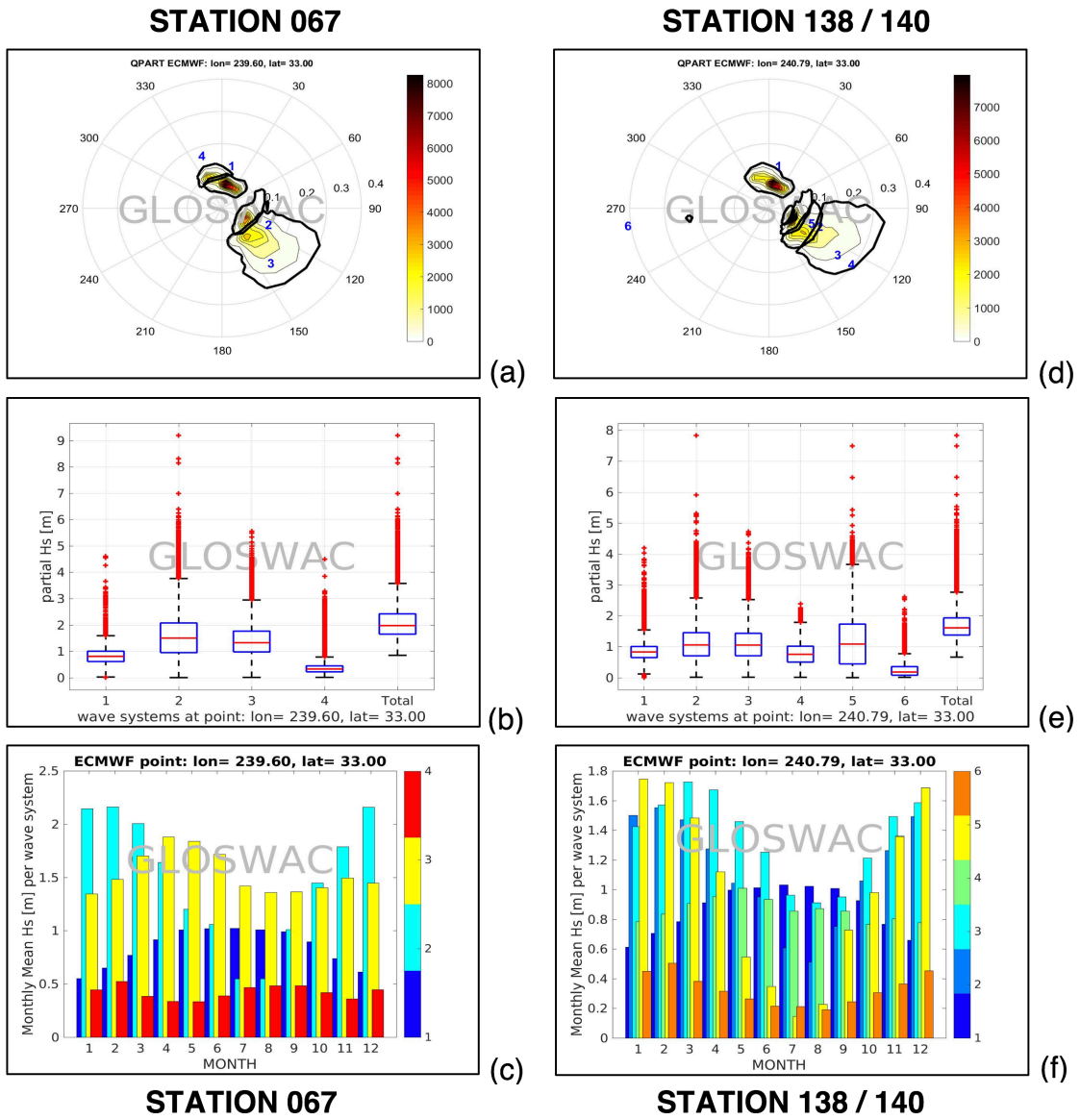


Figure 13. GLOSWAC plots corresponding to CDIP Stations 067, 138, and 140.

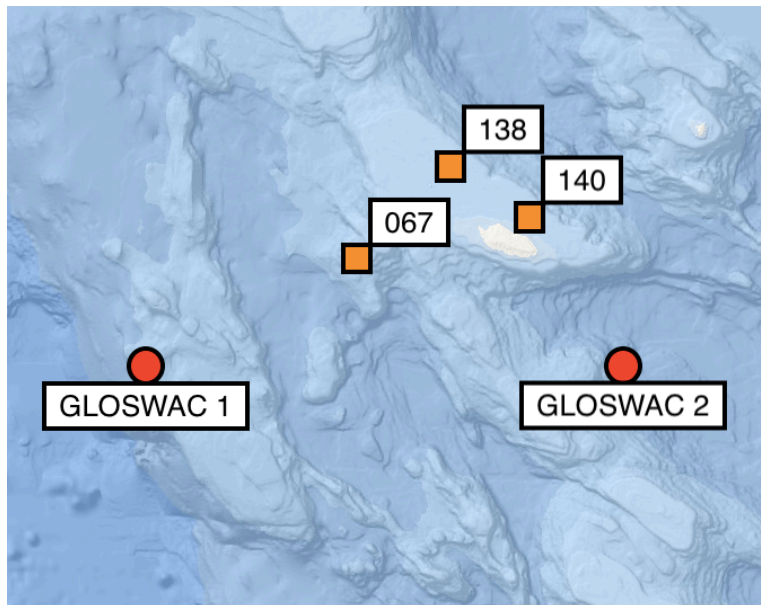


Figure 14. Map of GLOSWAC data points and CDIP buoys

The GLOSWAC “Significant Wave Height Distribution Per Wave System” box and whisker plots (Figure 13b and e) show wave height distribution for each of the distinct wave systems partitioned in Figure 13a and d. The horizontal red line segments designate the median for that wave system, the box limits denote the 25th and 75th percentile range, the dashed whiskers extend 1.5 times the interquartile range, and the red data points show extreme values. The systems at Station 067 generally have greater significant median and extreme wave heights than at Stations 138 and 140, a trend supported by the observed CDIP buoy data. GLOSWAC sea state behavior at Station 140 is not in agreement with CDIP buoy data, but does agree with buoy data for Station 138. The failure of the GLOSWAC system to capture behavior at Station 140 raises concerns: wave spectra informing the GLOSWAC model have a grid resolution of approximately 100 km, and all three buoys are located within a 100-km square bounding San Nicolas Island. Nonetheless, the GLOSWAC plots remain informative when considering spectral partitioning and comparisons of the monthly-averaged wave height estimates to observed values.

The GLOSWAC “Monthly Mean Significant Wave Height” plots (Figure 13c and f) show the monthly-averaged significant wave heights for each partition labeled in Figure 13a and d. Comparing the model results (Figure 13c) with the observed monthly-averaged values for Station 067 (see Figure 6 or 10) shows that wave system 2, which principally contains waves from the northwest, dominates the waves at the site. Conducting the same comparison of model results (Figure 13f) with observed data for Station 138 shows that wave systems 2, 3, and 5 dominate, which also correspond to waves from the northwest. The same comparison of model results (Figure 13f) with

observed data for Station 140 is less clear. It appears that none of the systems fit the observed data well, and that perhaps wave system 4 (Figure 13c), containing waves from the south, fits best.

5. SPATIAL GRADIENTS CASE STUDY

Spatial gradients were calculated for significant wave height and energy period between offshore SWIFT (Surface Wave Instrument Float with Tracking) buoy locations and CDIP buoy locations near San Nicolas Island [9]. Comparisons were made between the observed data (SWIFT and CDIP) and the data available from the NREL atlas at the same locations as the SWIFT and CDIP buoys.

In general, the NREL atlas underestimates slightly the observed spatial gradients for significant wave height and fails to capture observed spatial gradients for energy period.

5.1 Gradient Comparison Methodology

Data were collected using four SWIFT drifters deployed on 17–20 March 2015. SWIFT drifters were grouped geographically. The SWIFT spatial coupling prompted averaging of their data into two sets, one corresponding to Location A and the other to Location B (Figure 15). Note that Station 140 was not operational in March 2015 and thus not used for any aspect of this analysis.

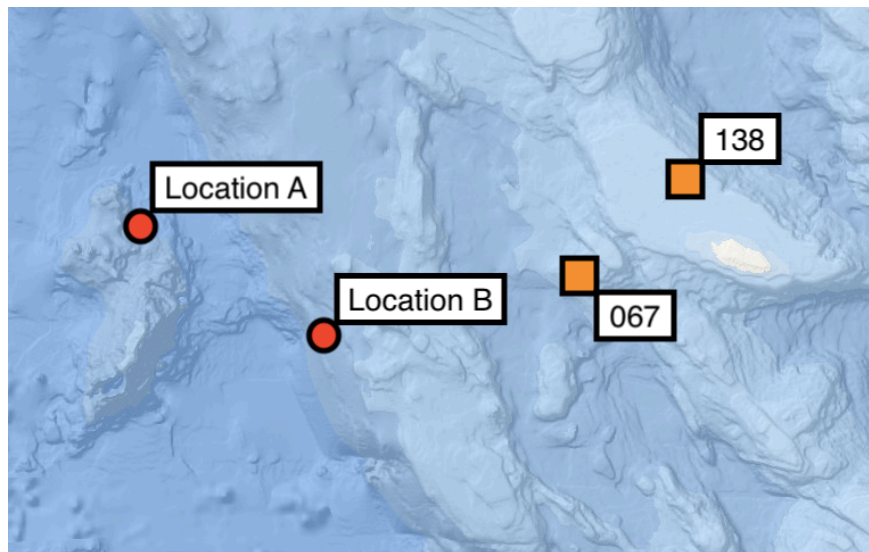


Figure 15. Map of SWIFT groupings and CDIP buoy stations.

Data for Locations A and B consist of averages of the appropriate SWIFT geographic coordinates and significant wave heights. To compare NREL atlas values, which only report the energy period, the energy period was calculated from each

SWIFT's data, averaged over all SWIFT data sets, then averaged across the appropriate SWIFT drifters to create values for Locations A and B.

Atlas data were gathered by retrieving the significant wave height and energy period from the NREL atlas for Location A, Location B, and the locations of Station 067 and Station 138 for the month of March 2015 by referencing bathymetry at the desired coordinates.

CDIP buoy data were trimmed to the time interval corresponding to the longest SWIFT deployment at each location. Significant wave height and energy period recorded by the CDIP buoys were averaged over the trimmed intervals.

Spatial gradient ratios were calculated for significant wave height and energy period from offshore to nearshore, and the results from observed data and the NREL atlas values were compared. The observed data consist of offshore SWIFT buoy measurements and nearshore CDIP buoy measurements. The observed spatial gradients were calculated by dividing the SWIFT measurements by the CDIP station measurements. Using values sourced from the NREL atlas, spatial gradients were calculated by dividing the atlas value at the SWIFT location by the atlas value at the CDIP station location.

5.2 Sea State During SWIFT Deployment

Before comparing spatial gradients between offshore and nearshore locations, it is important to consider whether data from the 17–20 March 2015 deployment represent data for the month of March averaged over several years. To determine if the date range is typical, the average significant wave heights and energy periods measured by CDIP buoys over this date range were plotted with the monthly-averaged values from the same CDIP buoys (Figure 16)

Sea state during the SWIFT deployment was generally representative of the typical sea state during March. The sea state during the SWIFT deployment had slightly greater wave heights and slightly shorter energy periods than typical. The range of values for significant wave height recorded by CDIP buoys during the SWIFT deployment is within one standard deviation of the typical sea state. The range of values for energy period recorded by CDIP buoys during the SWIFT deployment extends beyond one standard deviation of the typical sea state. Although these parameter variations should be noted, SWIFT gradients can be calculated and discussed with confidence that the duration of the SWIFT deployment is generally representative of typical sea states during March.

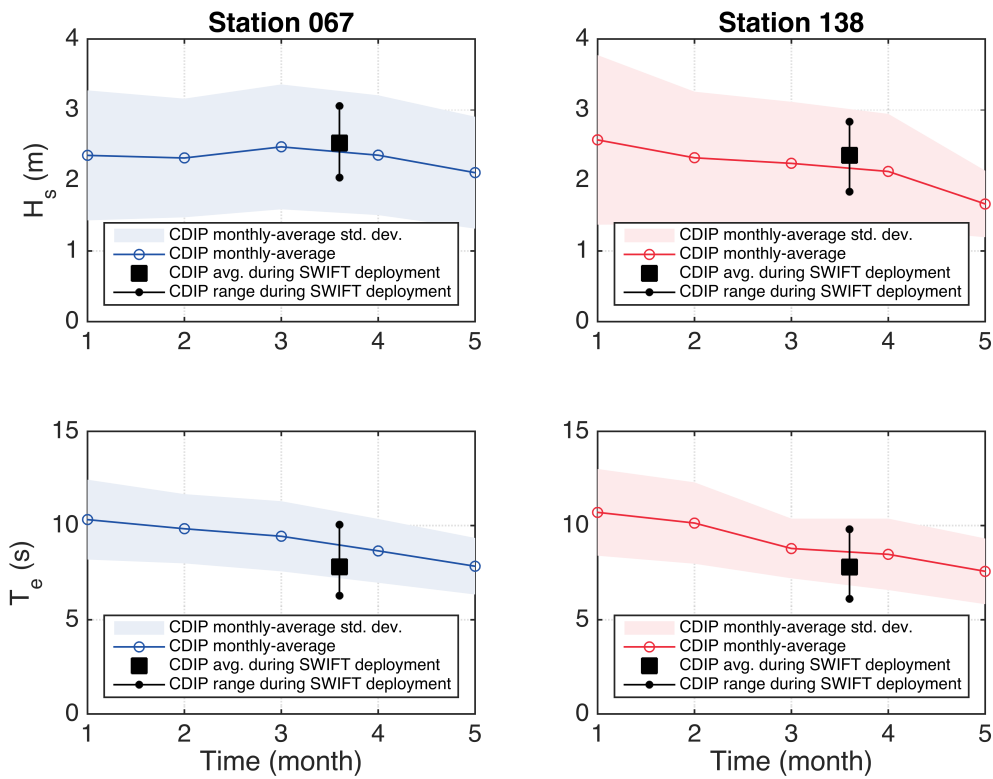


Figure 16. Typicality of sea state during SWIFT deployment on 17–20 March 2015 near San Nicholas Island

5.3 Spatial Gradient Comparison: Significant Wave Height

Spatial gradient ratios for significant wave height are reported as the value $H_{\text{swift}}/H_{\text{stn}}$, the observed spatial gradient calculated by dividing observed data offshore at a SWIFT location by observed data nearshore at a CDIP buoy, and the value $H_{\text{atlas@swift}}/H_{\text{atlas@stn}}$, the atlas spatial gradient calculated by dividing the atlas data for March at the SWIFT location by atlas data for March at the CDIP buoy location.

The spatial gradients (Table 3) reflect how many times greater significant wave height was at the locations of the deployed SWIFTS than at the CDIP buoy locations. The ratios are calculated for both the observed data and the atlas data to draw conclusions about the usefulness of the NREL wave atlas spatial gradients.

Table 3. Significant wave height spatial gradients comparison

	Station 067		Station 138	
	$H_{\text{swift}} / H_{\text{stn}}$	$H_{\text{atlas@swift}} / H_{\text{atlas@stn}}$	$H_{\text{swift}} / H_{\text{stn}}$	$H_{\text{atlas@swift}} / H_{\text{atlas@stn}}$
Location A	1.15	1.07	1.24	1.21
Location B	1.08	1.06	1.16	1.20

The observed significant wave height gradient for SWIFT Location A and Station 067 is 1.15, meaning that observed wave heights offshore at Location A are 15% greater than wave heights at Station 067. The decrease in wave height from offshore to nearshore is opposite that expected from shoaling. Instead, this is likely due to large-scale refraction in the Southern California bight. As waves approach the coast, the shore-normal component of energy flux is conserved, while the along-shore component continues to travel along the shore. The SWIFT buoys and CDIP buoys experience similar shore-normal energy flux, but because the SWIFT buoys were deployed further offshore, they experienced a greater along-shore component. The decreased along-shore component of energy flux experienced by the CDIP buoys results in smaller waves than those experienced by the SWIFT buoys.

The ratio of the NREL atlas wave height at Location A to the atlas wave height at Station 067 is 1.07, meaning that waves offshore at Location A (according to the atlas) are 7% higher than waves at Station 067 (also according to the atlas). The gradients based on observed data and atlas data are in reasonable agreement. The observed data show 15% greater H_s offshore, while the atlas shows 7% greater H_s offshore. The smaller ratio for atlas data suggests that the atlas is unable to fully reflect spatial gradients, at least for Location A and Station 067.

The ratio of observed wave height at Location A to wave height at Station 138 is 1.24, meaning that waves offshore at Location A as measured by SWIFTs are 24% greater than waves observed over the same dates at Station 138. The primary explanation for this ratio is the same as described above. This ratio might be larger than the same ratio for Station 067 because Station 138 is closer to the coast, experiences lower wave heights, and thus yields a larger ratio.

The atlas gradient for Station 138 is 1.21 and matches well the observed gradient, showing that the atlas appears to perform reasonably well in characterizing spatial gradients for the locations corresponding to Station 138 and Location A.

Similar ratios were calculated for Location B. The ratios are all slightly less than their respective ratios at Location A. This difference between Location A and Location B is likely due to the closer geographic proximity of Location B to the buoy stations (Figure 15). The similarity of Location B and station observations yield smaller ratios. Because the atlas gradients for Locations A and B are more similar than the observed gradients, it

suggests that the atlas does not distinguish between Locations A and B as well as the observed measurements.

5.4 Spatial Gradient Comparison: Energy Period

Spatial gradient ratios for energy period are reported as the value $T_{\text{swift}}/T_{\text{stn}}$, the observed spatial gradient calculated by dividing observed data offshore at a SWIFT location by observed data nearshore at a CDIP buoy, and the value $T_{\text{atlas@swift}}/T_{\text{atlas@stn}}$, the atlas spatial gradient calculated by dividing the atlas data for March at the SWIFT location by atlas data for March at the CDIP buoy location.

The ratios (Table 4) reflect how many times greater energy periods are at the locations of the deployed SWIFTs than at the CDIP buoys. The ratios are calculated for both the SWIFT data and the atlas data to draw conclusions about the usefulness of using the NREL wave atlas to acquire information about spatial gradients in wave parameters.

Table 4. Energy period spatial gradients comparison

	Station 067		Station 138	
	$T_{\text{swift}} / T_{\text{stn}}$	$T_{\text{atlas@swift}} / T_{\text{atlas@stn}}$	$T_{\text{swift}} / T_{\text{stn}}$	$T_{\text{atlas@swift}} / T_{\text{atlas@stn}}$
Location A	0.88	0.98	0.88	0.99
Location B	0.87	0.99	0.87	0.99

It is immediately apparent that the ratio of magnitudes for the energy period spatial gradients are all similar. The observed spatial gradients are all less than one, and are similar in magnitude at Locations A and B. With observed gradients less than one, the energy period calculated for the SWIFT locations is less than the energy period measured by the CDIP buoys, which may be due to the broader distribution of periods at the SWIFT locations than at the CDIP buoys. The large-scale refraction may allow longer wavelength systems to reach nearshore locations and local winds may broaden the spectrum.

Both the observed and atlas gradients are nearly identical for CDIP station locations and SWIFT locations, suggesting that there is little variation between offshore and nearshore locations.

The atlas gradients are nearly 1, indicating that the atlas depicts little change in energy period from offshore to nearshore locations. This contrasts with the observed gradients, where the energy period becomes longer at nearshore locations.

6. REFERENCES

1. M. Folley, The wave energy resource. In: *Handbook of Ocean Wave Energy*, A. Pecher and J. Kofoed, eds., 43-79 (Springer, 2017).
2. U.S. Army Corps of Engineers, *Coastal Engineering Manual*. (Washington, D.C, 2006).
3. P.T. Jacobson, G. Hagerman, and G. Scott, *Mapping and Assessment of the United States Ocean Wave Energy Resource*. Electric Power Research Institute, Technical Report 1024637, December 2011.
4. National Research Council, Committee on Marine Hydrokinetic Energy Technology Assessment, *An evaluation of the U.S. Department of Energy's Marine and Hydrokinetic Resource Assessments*. (Washington, D.C.: National Academies Press, 2013).
5. The Crown Estate, Black & Veatch Ltd., *U.K. Wave and Tidal Key Resource Areas Project*. Technical Methodology Report, February 2013.
6. NOAA, National Weather Service, Climate Prediction Center, *Cold and Warm Episodes by Season*. Retrieved from: http://origin.cpc.ncep.noaa.gov/products/analysis_monitoring/ensostuff/ONI_v5.php
7. J. Thomson, E. D'Asaro, M. Cronin, E. Rogers, R. Harcourt, and A. Shcherbina, Waves and the equilibrium range at Ocean Weather Station P. *J. Geophys. Res.*, 118, 5951-5962, 2013.
8. J. Portilla-Yandún, The global signature of ocean wave spectra. *Geophys. Res. Lett.*, 45, 267-276, 2018.
9. J. Thomson, Wave breaking dissipation observed with SWIFT drifters. *J. Atmos. Ocean. Technol.*, 29, 1866-1882, 2012.

7. APPENDIX: ACCESSING DATA FROM THREDDS SERVER AND CDIP WEBSITE IN MATLAB

The procedure for setting up and beginning use with the THREDDS server was primarily learned from an example script from CDIP, found here:

https://cdip.ucsd.edu/themes/media/docs/documents/html_pages/spectrum_plot_matlab.txt

The pre-code setup instructions are as follows:

1. Download the nctoolbox from: <https://github.com/nctoolbox>
2. Download and extract into a folder
3. Open MATLAB and at the MATLAB prompt cd to the extracted folder where setup_nctoolbox lives
4. Run setup_nctoolbox

The code used to import data and take the mean for this report is as follows:

```

%%%%%%%%%%%%%%%%%%%%%%%%%%%%%%%%%%%%%%%%%%%%%%%%%%%%%%%%%%%%%%%%%%%%%%%%
%CHANGE DIRECTORY TO 'NCTOOLBOX' DIRECTORY

cd nctoolbox-master

% OPEN NCTOOLBOX IN MATLAB

setup_nctoolbox

% RETURN TO DESIRED FOLDER

cd
/Users/noahjohnson/Dropbox/SanNicolasIsland/NoahResults/Spectra

% USER ENTERS STATION NUMBER

stn = {'067','138'};

for j = 1:length(stn)

```

```
% CONNECT TO THREDDS SERVER AND OPEN NETCDF FILE

urlbase =
'http://thredds.cdip.ucsd.edu/thredds/dodsC/cdip/archive/'; %
Set 'base' THREDDS URL and pieces to concatenate with user-
defined station number (set above)

p1 = 'p1/';
urlend = 'p1_historic.nc';
dsurl = strcat(urlbase,stn{j},p1,stn{j},urlend);
ds = ncdataset(dsurl);

% PRINT LIST OF VARIABLES IN NETCDF FILE

% varlist = ds.variables

% GET BUOY NAME AND TRANSPOSE TO HORIZONTAL STRING

buoyname = ds.data('metaStationName');

buoytitle = transpose(buoyname(1:end-2)); % 'end-2' omits
'set' field i.e. "p1"

% CALL TIME VARIABLE

timeUNIX = ds.data('waveTime'); % apparently given in UNIX
timestamps (?)

timeSer = ds.time('waveTime',timeUNIX); % Convert UNIX
timestamps to Matlab serial units

timeVec = datevec(timeSer); % convert from serial to vector

% GET SPECTRA DATA
```

```

    Ed = ds.data('waveEnergyDensity'); % get energy density
data, transpose

    valFq = ds.data('waveFrequency'); % get frequency values
(single column)

    Fq = repmat(valFq,1,length(Ed)); % repeat frequency vector to
create matrix same size as Ed

% GET BULK PARAMETER DATA

Hs = ds.data('waveHs');
Tp = ds.data('waveTp');
Ta = ds.data('waveTa');

% CALCULATE ENERGY PERIOD FOR ALL SPECTRA

energyFreq = sum(Ed.*Fq)./sum(Ed); % Integrating (f*E(f)*df)
/ (E(f)*df) to find energy frequency

energyPeriod = 1./energyFreq; % Taking inverse of energy
frequency to find energy period

% AVERAGE SPECTRA BY MONTH

for i = 1:12; %loop over months

    idx = find(timeVec(:,2)==i); % find all indices for the
specific month

    meanEd(:,i) = mean(Ed(:,idx),2); % calculate mean Ed for each
frequency bin for spectra that are from the i-th month

    meanTe(:,i) = mean(energyPeriod(idx)); % calculate mean Te
from spectra that are from the i-th month

end

```

```

% CREATE STRUCTURE OF DATA AND SAVE

spcData(j).name = buoytitle;
spcData(j).station = stn{j};
spcData(j).time = timeVec;
spcData(j).Ed = Ed;
spcData(j).freq = Fq;
spcData(j).monthEd = meanEd;
spcData(j).monthTe = meanTe;
spcData(j).Te = energyPeriod;
spcData(j).Hs = Hs;
spcData(j).Tp = Tp;
spcData(j).Ta = Ta;

end

save('spcData','spcData')

%%%%%%%%%%%%%%%%%%%%%%%%%%%%%%%%%%%%%%%%%%%%%%%%%%%%%%%%%%%%%%%%%%%%%%%%

```

Data from Station 140 was not accessible from the THREDDDS server and it was thus necessary to download ‘sp’ files directly from the CDIP website. Station 140 was accessed here:

http://cdip.ucsd.edu/?nav=historic&sub=data&units=metric&tz=UTC&pub=public&map_stati=1,2,3&stn=140&stream=p1

To access the downloaded files, follow these steps:

1. Navigate to the above URL
2. Select any of the blue ‘E’ links
3. Select ‘All Types’ under the ‘Download’ section on the side bar
4. Select the time range 1991/01/01 to 1994/01/01 to capture all available data

5. Select the 'Spectra' link under the 'Sensor01' tab in the table

Because some of the spectra sets in the data file (seemingly randomly) switching from 128 samples to 64 samples, these 64-band data sets were removed manually from the text file and were not considered in the analysis presented here.

To read the data from the text file to a useable format, the 'read_cdip_buoy' MATLAB function was used to structure the data with the following script after removing problem data sets:

```

%%%%%%%%%%%%%%%%%%%%%%%%%%%%%%%%%%%%%%%%%%%%%%%%%%%%%%%%%%%%%%%%%%%%%%%%
file = 'sp140p101_199101010000-199401012359';
tmestr = 'all';
[spc,sys]=read_cdip_buoy(file,tmestr);
%%%%%%%%%%%%%%%%%%%%%%%%%%%%%%%%%%%%%%%%%%%%%%%%%%%%%%%%%%%%%%%%%%%%%%%%

```

The data for station 140 was then incorporated into the existing structure that included stations 067 and 138:

```

%%%%%%%%%%%%%%%%%%%%%%%%%%%%%%%%%%%%%%%%%%%%%%%%%%%%%%%%%%%%%%%%%%%%%%%%
cd
/Users/noahjohnson/Dropbox/SanNicolasIsland/NoahResults/Spectra
load('spcData.mat')
load('140spcData.mat')

% CONVERT STATION 140 TIME DATA
timeVec = datevec(sys.tme); % convert from serial to vector

% GET STATION 140 SPECTRA DATA
Ed = spc.en; % get energy density data
Fq = spc.fr; % get frequency data

```

```
% GET BULK PARAMETER DATA

Hs = sys.Hs;

Tp = sys.Tp;

Ta = sys.Ta;

% CALCULATE ENERGY PERIOD FOR ALL SPECTRA

energyFreq = sum(Ed.*Fq)./sum(Ed); % Integrating (f*E(f)*df)
/ (E(f)*df) to find energy frequency

energyPeriod = 1./energyFreq; % Taking inverse of energy
frequency to find energy period

% AVERAGE SPECTRA BY MONTH

for i = 1:12; %loop over months

    idx = find(timeVec(:,2)==i); % find all indices for the
specific month

    meanEd(:,i) = mean(Ed(:,idx),2); % calculate mean Ed for each
frequency bin for spectra that are from the i-th month

    meanTe(:,i) = mean(energyPeriod(idx)); % calculate mean Te
from spectra that are from the i-th month

end

% ADD STATION 140 DATA INTO EXISTING 'spcData' structure

spcData(3).name = 'SAN NICOLAS ISLAND BARGE LANDING BUOY -
140';

spcData(3).station = '140';

spcData(3).time = timeVec;
```

```
spcData(3).Ed = Ed;  
spcData(3).freq = Fq;  
spcData(3).monthEd = meanEd;  
spcData(3).monthTe = meanTe;  
spcData(3).Te = energyPeriod;  
spcData(3).Hs = Hs;  
spcData(3).Tp = Tp;  
spcData(3).Ta = Ta;  
  
% % SAVE NEW STRUCTURE 'spcData'  
save('spcData','spcData')  
%%%%%%%%%%%%%%%%%%%%%%%%%%%%%%%%%%%%%%%%%%%%%%%%%%%%%%%%%%%%%%%%%%%%%%%%
```

REPORT DOCUMENTATION PAGE

*Form Approved
OMB No. 0704-0188*

The public reporting burden for this collection of information is estimated to average 1 hour per response, including the time for reviewing instructions, searching existing data sources, gathering and maintaining the data needed, and completing and reviewing the collection of information. Send comments regarding this burden estimate or any other aspect of this collection of information, including suggestions for reducing the burden, to Department of Defense, Washington Headquarters Services, Directorate for Information Operations and Reports (0704-0188), 1215 Jefferson Davis Highway, Suite 1204, Arlington, VA 22202-4302. Respondents should be aware that notwithstanding any other provision of law, no person shall be subject to any penalty for failing to comply with a collection of information if it does not display a currently valid OMB control number.

PLEASE DO NOT RETURN YOUR FORM TO THE ABOVE ADDRESS.

1. REPORT DATE (DD-MM-YYYY)			2. REPORT TYPE		3. DATES COVERED (From - To)	
4. TITLE AND SUBTITLE				5a. CONTRACT NUMBER		
				5b. GRANT NUMBER		
				5c. PROGRAM ELEMENT NUMBER		
6. AUTHOR(S)				5d. PROJECT NUMBER		
				5e. TASK NUMBER		
				5f. WORK UNIT NUMBER		
7. PERFORMING ORGANIZATION NAME(S) AND ADDRESS(ES)				8. PERFORMING ORGANIZATION REPORT NUMBER		
9. SPONSORING/MONITORING AGENCY NAME(S) AND ADDRESS(ES)				10. SPONSOR/MONITOR'S ACRONYM(S)		
				11. SPONSOR/MONITOR'S REPORT NUMBER(S)		
12. DISTRIBUTION/AVAILABILITY STATEMENT						
13. SUPPLEMENTARY NOTES						
14. ABSTRACT						
15. SUBJECT TERMS						
16. SECURITY CLASSIFICATION OF:			17. LIMITATION OF ABSTRACT	18. NUMBER OF PAGES	19a. NAME OF RESPONSIBLE PERSON	
a. REPORT	b. ABSTRACT	c. THIS PAGE			19b. TELEPHONE NUMBER (Include area code)	

INSTRUCTIONS FOR COMPLETING SF 298

1. REPORT DATE. Full publication date, including day, month, if available. Must cite at least the year and be Year 2000 compliant, e.g. 30-06-1998; xx-06-1998; xx-xx-1998.

2. REPORT TYPE. State the type of report, such as final, technical, interim, memorandum, master's thesis, progress, quarterly, research, special, group study, etc.

3. DATES COVERED. Indicate the time during which the work was performed and the report was written, e.g., Jun 1997 - Jun 1998; 1-10 Jun 1996; May - Nov 1998; Nov 1998.

4. TITLE. Enter title and subtitle with volume number and part number, if applicable. On classified documents, enter the title classification in parentheses.

5a. CONTRACT NUMBER. Enter all contract numbers as they appear in the report, e.g. F33615-86-C-5169.

5b. GRANT NUMBER. Enter all grant numbers as they appear in the report, e.g. AFOSR-82-1234.

5c. PROGRAM ELEMENT NUMBER. Enter all program element numbers as they appear in the report, e.g. 61101A.

5d. PROJECT NUMBER. Enter all project numbers as they appear in the report, e.g. 1F665702D1257; ILIR.

5e. TASK NUMBER. Enter all task numbers as they appear in the report, e.g. 05; RFO330201; T4112.

5f. WORK UNIT NUMBER. Enter all work unit numbers as they appear in the report, e.g. 001; AFAPL30480105.

6. AUTHOR(S). Enter name(s) of person(s) responsible for writing the report, performing the research, or credited with the content of the report. The form of entry is the last name, first name, middle initial, and additional qualifiers separated by commas, e.g. Smith, Richard, J, Jr.

7. PERFORMING ORGANIZATION NAME(S) AND ADDRESS(ES). Self-explanatory.

8. PERFORMING ORGANIZATION REPORT NUMBER. Enter all unique alphanumeric report numbers assigned by the performing organization, e.g. BRL-1234; AFWL-TR-85-4017-Vol-21-PT-2.

9. SPONSORING/MONITORING AGENCY NAME(S) AND ADDRESS(ES). Enter the name and address of the organization(s) financially responsible for and monitoring the work.

10. SPONSOR/MONITOR'S ACRONYM(S). Enter, if available, e.g. BRL, ARDEC, NADC.

11. SPONSOR/MONITOR'S REPORT NUMBER(S). Enter report number as assigned by the sponsoring/monitoring agency, if available, e.g. BRL-TR-829; -215.

12. DISTRIBUTION/AVAILABILITY STATEMENT. Use agency-mandated availability statements to indicate the public availability or distribution limitations of the report. If additional limitations/ restrictions or special markings are indicated, follow agency authorization procedures, e.g. RD/FRD, PROPIN, ITAR, etc. Include copyright information.

13. SUPPLEMENTARY NOTES. Enter information not included elsewhere such as: prepared in cooperation with; translation of; report supersedes; old edition number, etc.

14. ABSTRACT. A brief (approximately 200 words) factual summary of the most significant information.

15. SUBJECT TERMS. Key words or phrases identifying major concepts in the report.

16. SECURITY CLASSIFICATION. Enter security classification in accordance with security classification regulations, e.g. U, C, S, etc. If this form contains classified information, stamp classification level on the top and bottom of this page.

17. LIMITATION OF ABSTRACT. This block must be completed to assign a distribution limitation to the abstract. Enter UU (Unclassified Unlimited) or SAR (Same as Report). An entry in this block is necessary if the abstract is to be limited.